Numerical study of the fluid flow and interface deflection for crystals grown by Bridgman technique

Simina Maris and Liliana Braescu

***Abstract*—A stationary, free boundary model describing the process of crystal growth in a vertical Bridgman installation is considered. For this model, the influence of the temperature profile in the furnace and gravitational field on the fluid flow and interface deflection, are investigated numerically by finite element method through FreeFem++ software.**

***Index Terms*—Free boundary problem, Stationary problem, Temperature profile, Interface deflection, Vertical Bridgman, Gravitational field, Numerical simulation**

I. Introduction

The Bridgman technique is a popular method of growing single crystals from compound materials that contain a volatile element. This is the case of the entire group III-V and II-VI semiconductor crystals. The method consists in movement of a crucible (ampoule), charged with powder and a seed, through a temperature gradient. The ampoule is introduced in the hot region of the furnace until the powder is melted, and then it is pulled with a rate $\bar{u}_{translation}$, such that it enters into the cold region and the solidification process begins [1].

The factors that influence the quality of the resulting crystal are:

- the temperature gradient in the furnace;
- the gravitational field;
- the properties of the material (e.g., specific heat, density, kinematic viscosity, thermal expansion coefficient, solidification temperature, initial dopant concentration);
- the ampoules velocity of translation in the furnace;
- the shape of solid-melt interface.

In the case of alloys for which equilibrium segregation coefficient of the dopant is less than unity, a serious problem is the amount of dopant rejected at the solid-melt interface. This quantity depends on the velocity field in melt and on the shape of solidification interface. Both these parameters depend on the value of the gravitational field and on the temperature profile inside the furnace.

In literature, there are several numerical investigations of the solidification process in vertical Bridgman installations ([2]-[11]).

Manuscript received September 16, 2010: Revised version received October 20, 2010.

This work was supported by the Romanian National University Research Council (CNCSIS-UEFISCU), project PNII-IDEI 131/2008.

S. Maris is with the Department of Computer Science, West University of Timisoara, Blv. V. Parvan 4, Timisoara, 300223, ROMANIA (corresponding author phone: +40-256-592-150; fax: +40-256-592-316; e-mail: smaris@info.uvt.ro).

L. Braescu is with the Computer Science Department, West University of Timisoara, Blv. V Parvan 4, Timisoara 300223, ROMANIA (e-mail: lilianabraescu@ balint1.math.uvt.ro).

In this paper, the dependence of fluid flow and interface deflection on the temperature profile are investigated numerically in a vertical Bridgman furnace, for various values of the gravitational field. The numerical simulations, based on a fixed-point algorithm, were performed using the FreeFem++ software.

II. Mathematical Formulation

Let us consider the stationary, free boundary model proposed in [3]. Because the crucible presents axial symmetry, the three-dimensional problem could be reduced to a two-dimensional one. Denoting by Ω_l the domain occupied by melt, Ω_s the domain occupied by crystal and the solidification interface by a function $h(r)$, we have [9]:

$$\Omega_s = \left\{(r,z) \in \mathbb{R}^2 \,|\, 0 < r < R \text{ and } 0 < z < h(r)\right\}$$
$$\Omega_l = \left\{(r,z) \in \mathbb{R}^2 \,|\, 0 < r < R \text{ and } h(r) < z < A\right\}$$
$$h(R) = \frac{A}{2}$$

A schematic representation of the computational domains is given in Figure 1, where $A = 1$ represents the dimensionless length of the ampoule, $R = 0.25$ is the dimensionless radius of the ampoule and L_g is the length of the gradient zone.

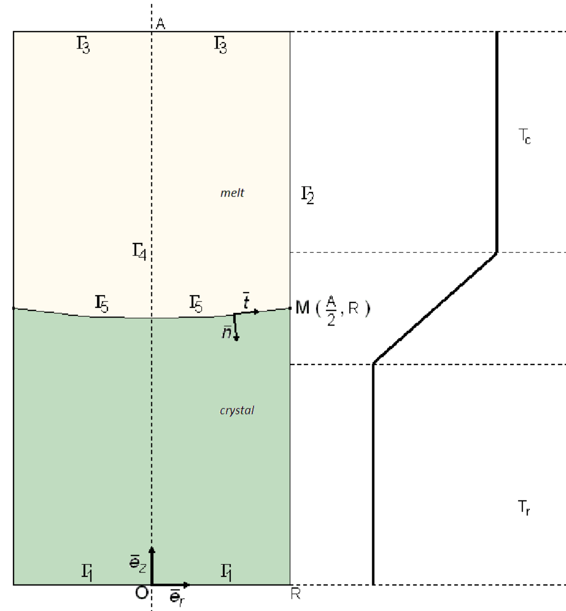

Fig. 1. The computational domains and the temperature profile inside the furnace

The translation of the ampoule inside the furnace is simulated by adding melt at $z = A$ and pulling crystal at $z = 0$.

The dimensionlss equations governing the process are

$$\begin{cases} \nabla \bar{u} = 0 \text{ in } \Omega_l \\ (\bar{u}\,\nabla)\,\bar{u} = -\nabla p + Pr\,\Delta\bar{u} + Ra\,Pr\,\theta\,\bar{\text{k}} \text{ in } \Omega_l \\ \bar{u}\,\nabla\theta = \Delta\theta \text{ in } \Omega_l \\ \bar{u}_c = -Pe\,\bar{\text{k}} \text{ in } \Omega_s \\ \bar{u}_c\,\nabla\theta_c = \gamma\,\Delta\theta_c \text{ in } \Omega_s \end{cases} \quad (1)$$

where $\bar{u}$ represents the dimensionless velocity of the melt; $\bar{u}_c$ - the dimensionless velocity of the crystal; θ - the dimensionless temperature of the melt; θ_c - the dimensionless temperature of the crystal; Ra (thermal Rayleigh number) defines the gravitational field ($Ra = 0$ for zero gravity, $Ra = 10^3$ for micro-gravity, $Ra = 10^6$ for normal gravity); $Pr = 0.01$ (Prandtl number) represents the dimensionless kinematic viscosity; $Pe = 0.01$ (Peclet number) represents the dimensionless translation velocity of the ampoule inside the furnace; $\gamma = 1$ is the ratio of solid and melt thermal diffusivities.

The boundary conditions are:

$$\bar{u}|_{\Gamma_2,\Gamma_3} = \bar{u}_{tr} \quad (2)$$

$$\bar{u}_c|_{\Gamma_1,\Gamma_2} = \bar{u}_{tr} \quad (3)$$

$$\bar{u}\cdot\bar{t}|_{\Gamma_5} = Pe\cdot t_z \quad (4)$$

$$\sigma(\bar{u}\cdot\bar{n})|_{\Gamma_5} = Pe\cdot n_z \quad (5)$$

$$\theta_c|_{\Gamma_1} = 0 \quad (6)$$

$$\theta|_{\Gamma_2} = \begin{cases} \dfrac{1}{L_g}z + \dfrac{L_g - A}{2L_g} & , z \in \left[\dfrac{A}{2}, \dfrac{A}{2} + \dfrac{L_g}{2}\right] \\ 1 & , z > \dfrac{A}{2} + \dfrac{L_g}{2} \end{cases} \overset{not}{=} \tau \quad (7)$$

$$\theta_c|_{\Gamma_2} = \begin{cases} 0 & , z < \dfrac{A}{2} - \dfrac{L_g}{2} \\ \dfrac{1}{L_g}z + \dfrac{L_g - A}{2L_g} & , z \in \left[\dfrac{A}{2} - \dfrac{L_g}{2}, \dfrac{A}{2}\right] \end{cases} \overset{not}{=} \tau_c \quad (8)$$

$$\theta|_{\Gamma_3} = 1 \quad (9)$$

$$\theta|_{\Gamma_5} = \theta_c|_{\Gamma_5} = 0.5 \quad (10)$$

$$[(\bar{n}\,\nabla\theta)_l - k\,(\bar{n}\,\nabla\theta)_s]_{\Gamma_5} = S\,Pe\,n_z \quad (11)$$

where $\bar{u}_{tr} = -0.01\bar{e}_z$ is the dimensionless velocity of translation of ampoule.

III. Numerical study of the fluid flow and interface deflection

The numerical simulations were performed using FreeFem++, software developped at Universite Pierre et Marie Curie, Paris [12], dedicated to solve nonlinear two-dimensional and three-dimensional partial differential equations, using the finite element method.

As one can observe from equations (7)-(8), the temperature profile in the furnace is considered a linear function on z-coordinate and depends by the length of the gradient zone, L_g. For investigating numerically the fluid flow and the shape of the fluid-melt interface, different values of L_g (from $L_g = \frac{1}{8}A$ to $L_g = A$) are considered, in the case of zero gravity, micro-gravity, respectively normal gravity conditions.

The free boundary is obtained from a fixed-point algorithm, presented in [10]. It takes as input data $h^{(0)}(r) = \dfrac{A}{2}$, $\bar{u}^{(0)}(r,z) = \bar{u}_{tr}$, $\theta^{(0)}(r,z) = \tau$, $\theta_c^{(0)}(r,z) = \tau_c$, and computes $h(r)$, $\bar{u}(r,z)$, $\theta(r,z)$, $\theta_c(r,z)$, as follows:

1) solve the heat equation with the boundary condition (11);
2) find the isotherm corresponding to (10);
3) construct a domain deformation in order to overlap the bounday to the isotherm found at the previous step;
4) solve the Navier-Stokes equation on the deformed domain;
5) repeat steps 1-4 until both variations of temperature field and velocity field become less than a sufficiently small value, ε.

A. Case of zero gravity

The zero gravity conditions ($Ra = 0$) imply that the body forces in the Navier-Stokes equation are zero. As a consequence, the temperature profile in the furnace does not influence the velocity field in the melt. The streamlines of the computed velocity field and temperature profile for different values of L_g in absence of gravity are plotted in Figs. 2-7.

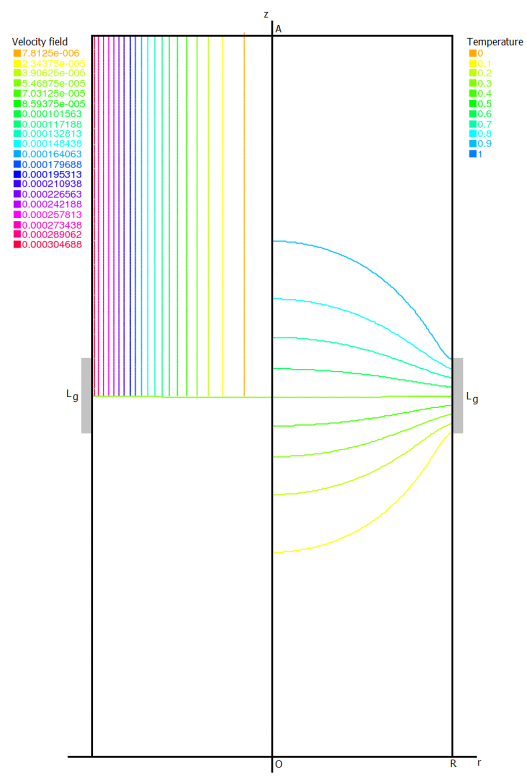

Fig. 2. Streamlines and temperature profile for $L_g = 0.125$, $Ra = 0$.

Figures show that the velocity fields present no convection cell, the movement of the melt being only determined by the

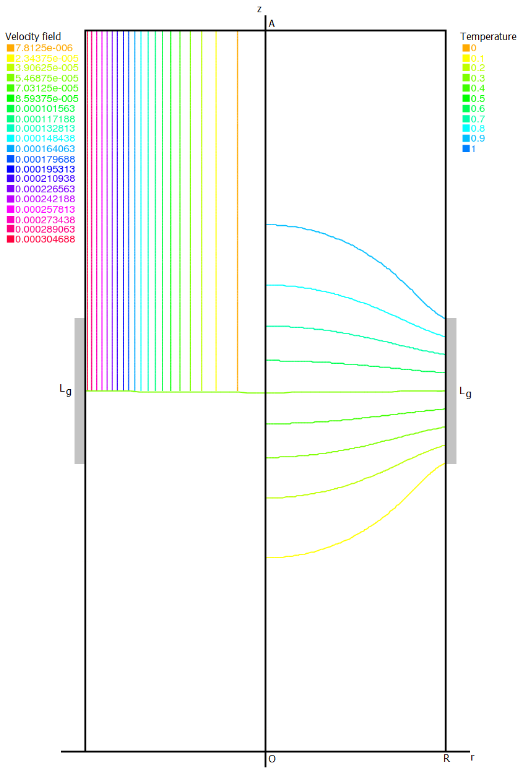

Fig. 3. Streamlines and temperature profile for $L_g = 0.250$, $Ra = 0$.

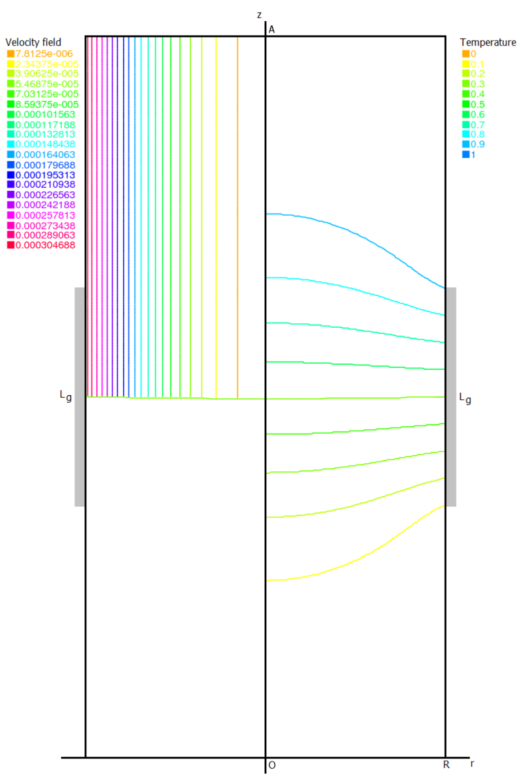

Fig. 4. Streamlines and temperature profile for $L_g = 0.375$, $Ra = 0$.

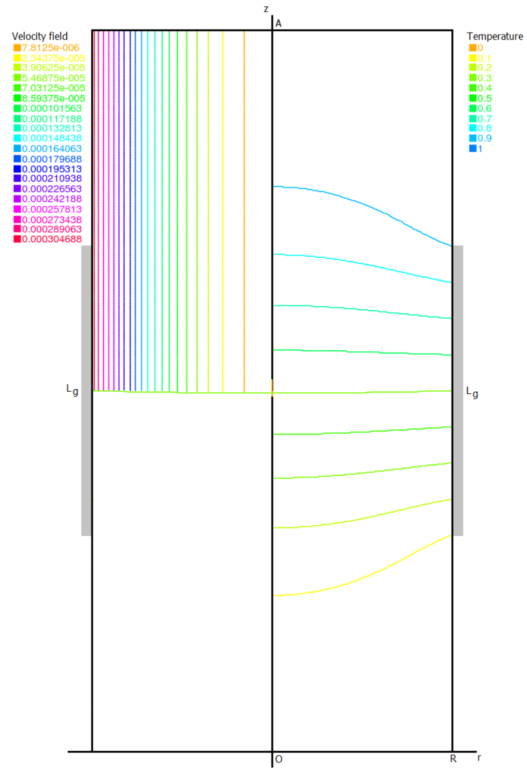

Fig. 5. Streamlines and temperature profile for $L_g = 0.500$, $Ra = 0$.

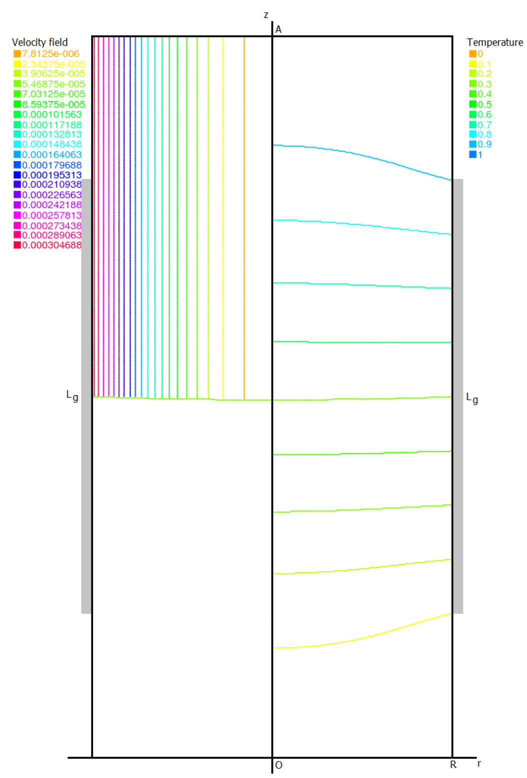

Fig. 6. Streamlines and temperature profile for $L_g = 0.750$, $Ra = 0$.

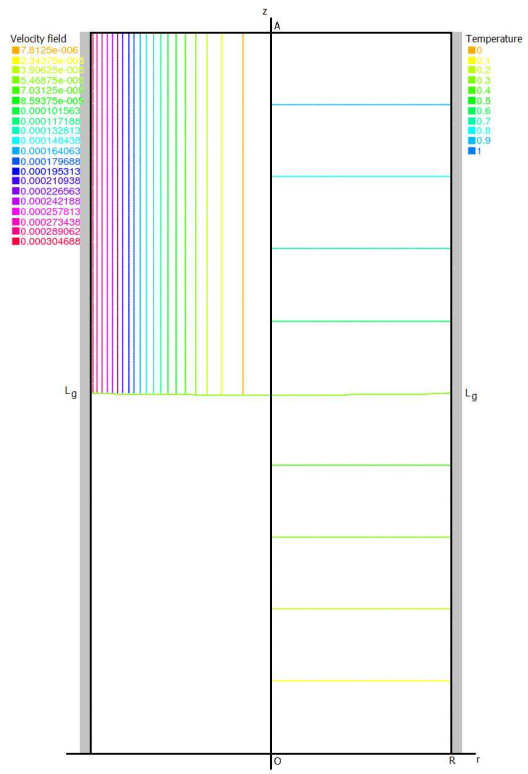

Fig. 7. Streamlines and temperature profile for $L_g = 1.000$, $Ra = 0$.

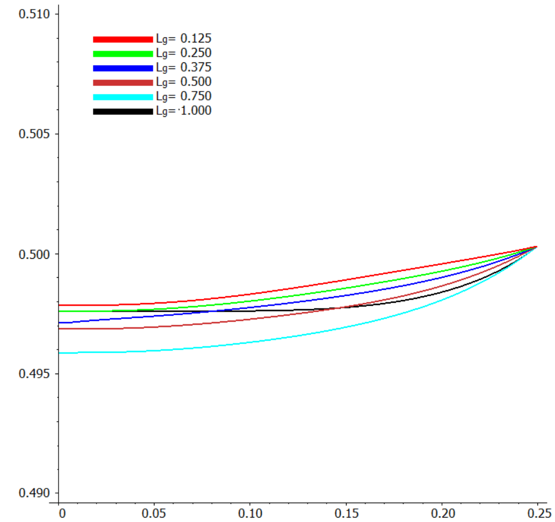

Fig. 8. The solidification interface corresponding to different values of L_g, for $Ra = 0$

TABLE I
MAXIMUM VALUE OF THE STREAMLINES OF THE FLUID FLOW FOR DIFFERENT L_g

L_g	Φ_{max} for $Ra = 0$
0.125	0.000304688
0.250	0.000304688
0.375	0.000304688
0.500	0.000304688
0.750	0.000304688
1.000	0.000304688

pulling rate, $\bar{u}_{tr}$. Also, the amplitude of the velocity field, Φ_{max}, does not depend on the length of the gradient zone (see Table I).

The deflection of the interface in zero gravity for the considered L_g is presented in Figure 8. This figure shows that variations of L_g in the range $[0.125, 1]$ produce small variations on the melt-solid interface. The solidification interface is a slight-convex shape and, for $L_g = 1$, it tends to be flatten.

B. Case of micro-gravity

In micro-gravity conditions ($Ra = 10^3$), the non-zero body forces in the Navier-Stokes equation determine a weak convection. Below, the computed streamlines in the melt and temperature inside the furnace obtained for different values of L_g in micro-gravity conditions are presented.

Figures 9-14 show that, in micro-gravity conditions, the velocity fields present a weak convection cell. Also, if the gradient zone increases from 0.125 to 1, then the streamlines

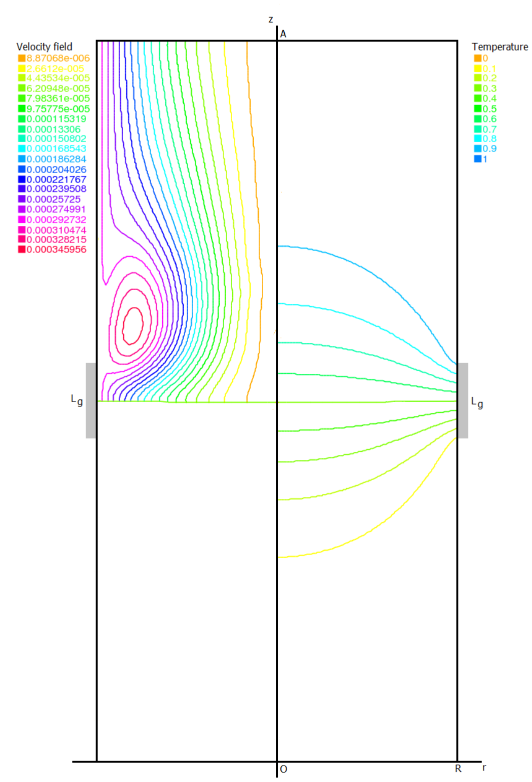

Fig. 9. Streamlines and temperature profile for $L_g = 0.125$, $Ra = 10^3$.

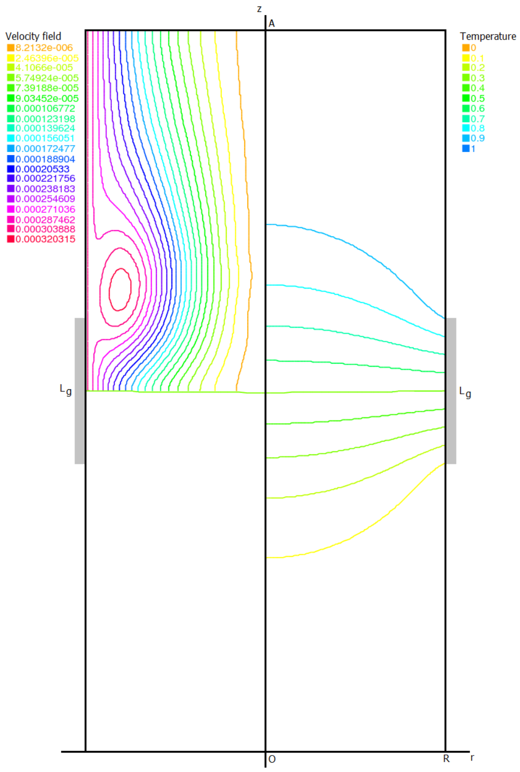

Fig. 10. Streamlines and temperature profile for $L_g = 0.250$, $Ra = 10^3$.

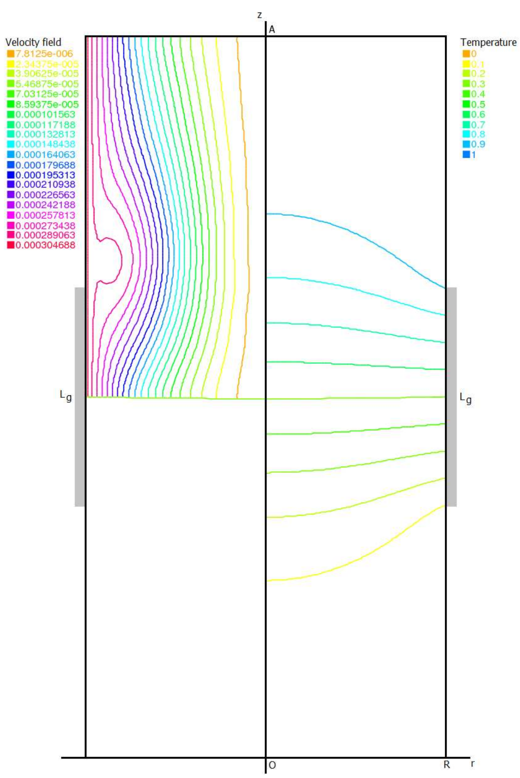

Fig. 11. Streamlines and temperature profile for $L_g = 0.375$, $Ra = 10^3$.

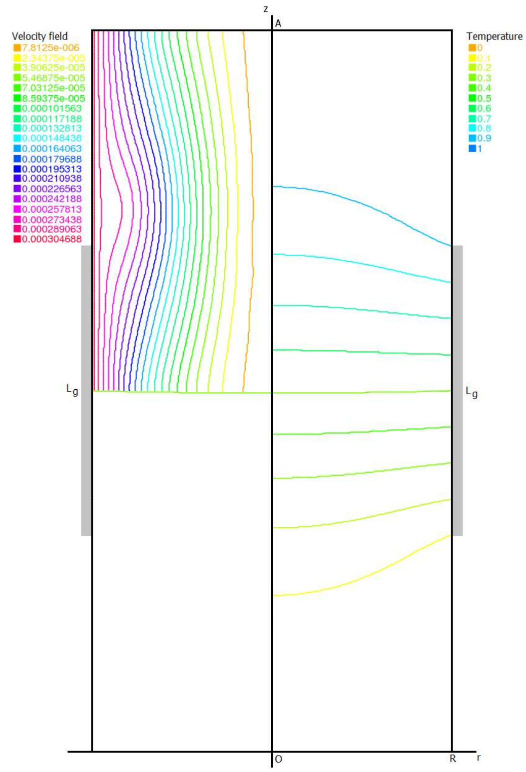

Fig. 12. Streamlines and temperature profile for $L_g = 0.500$, $Ra = 10^3$.

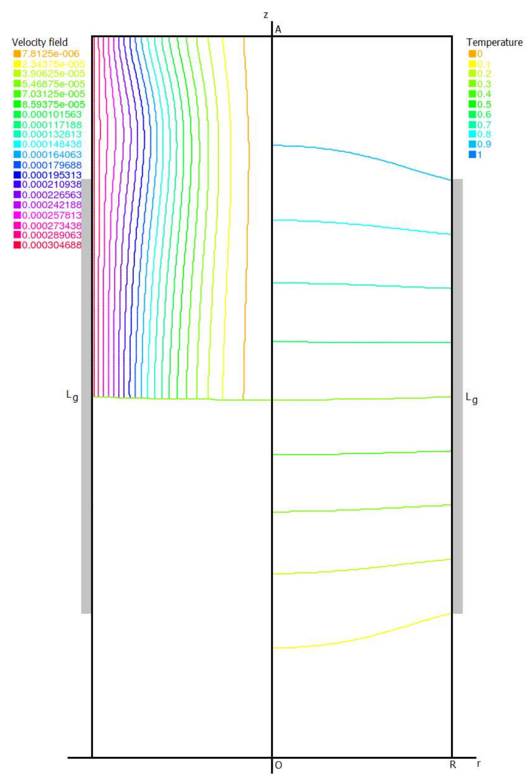

Fig. 13. Streamlines and temperature profile for $L_g = 0.750$, $Ra = 10^3$.

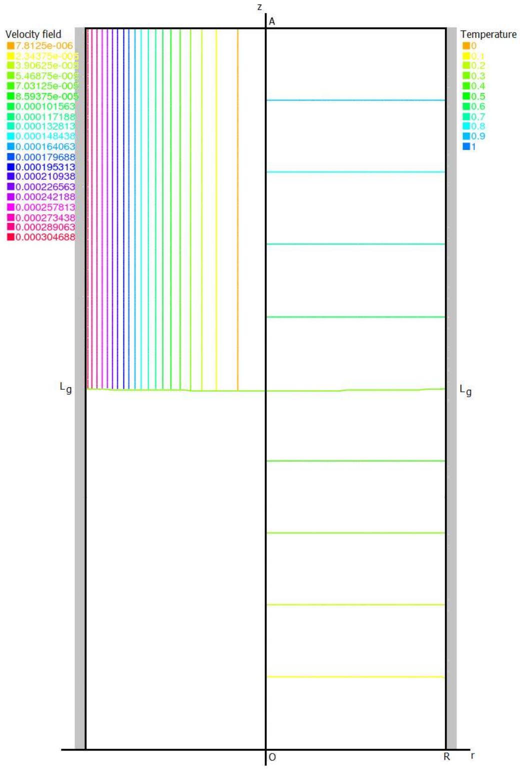

Fig. 14. Streamlines and temperature profile for $L_g = 1.000$, $Ra = 10^3$.

TABLE II
MAXIMUM VALUE OF THE STREAMLINES OF THE FLUID FLOW FOR DIFFERENT L_g

L_g	Φ_{max} for $Ra = 10^3$
0.125	0.000345956
0.250	0.000320315
0.375	0.000304688
0.500	0.000304688
0.750	0.000304688
1.000	0.000304688

of the fluid flow have a maximum situated above the gradient zone. These maxima decrease as L_g increases (see Table II).

The deflection of the interface for the considered L_g (see Figure 15) shows that variations of L_g in the range $[0.125, 1]$ produce small variations on the melt-solid interface, which preserve a slight-convex shape. If $L_g = 1$, then the interface shape tends to be flatten.

C. Case of normal gravity

In normal gravity conditions ($Ra = 10^6$), the body forces in the Navier-Stokes equation determine a strong convection. This alters both the shape of the velocity and temperature fields. The computed streamlines and temperature profiles, obtained for different values of the gradient zone length, L_g, are presented in Figs. 16-21.

Computations show that, in terrestrial gravity conditions, the velocity fields present a strong convection cell, which has a maximum situated above the gradient zone. These maxima decrease as L_g increases (see Table III).

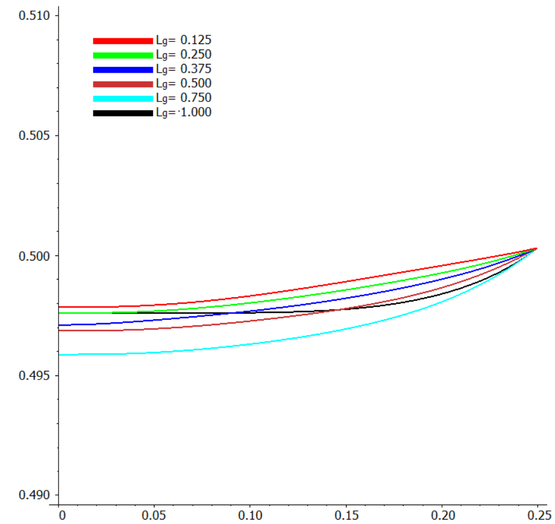

Fig. 15. The solidification interface corresponding to different values of L_g for $Ra = 10^3$

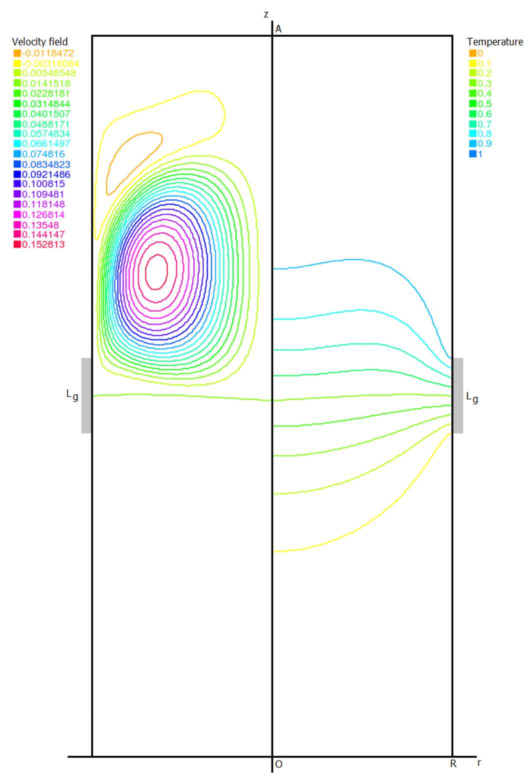

Fig. 16. Streamlines and temperature profile for $L_g = 0.125$, $Ra = 10^6$.

TABLE III
MAXIMUM VALUE OF THE STREAMLINES OF THE FLUID FLOW FOR DIFFERENT L_g

L_g	Φ_{max} for $Ra = 10^6$
0.125	0.152813
0.250	0.140295
0.375	0.123135
0.500	0.103699
0.750	0.0571388
1.000	0.000304688

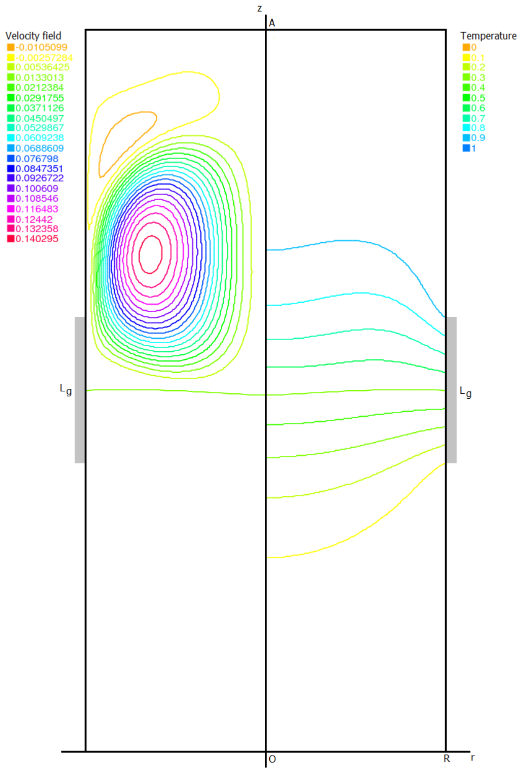

Fig. 17. Streamlines and temperature profile for $L_g = 0.250$, $Ra = 10^6$.

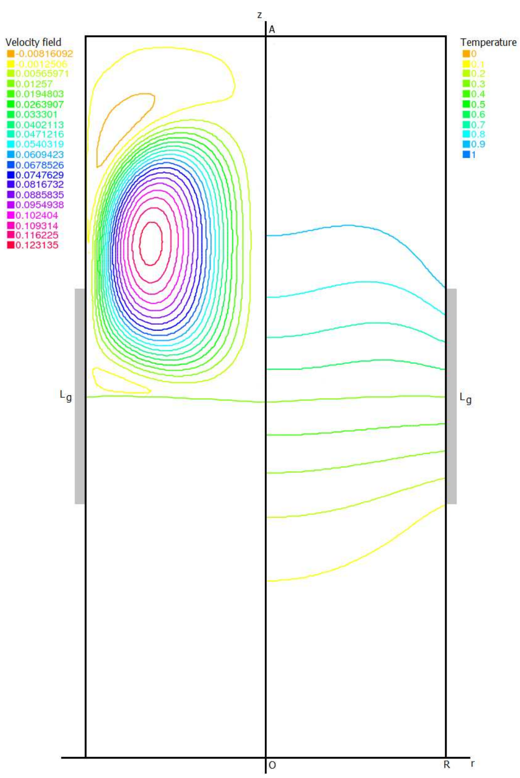

Fig. 18. Streamlines and temperature profile for $L_g = 0.375$, $Ra = 10^6$.

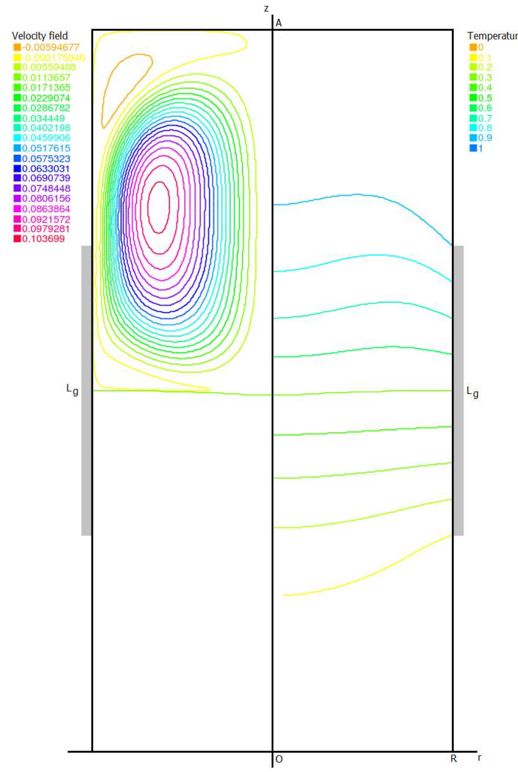

Fig. 19. Streamlines and temperature profile for $L_g = 0.500$, $Ra = 10^6$.

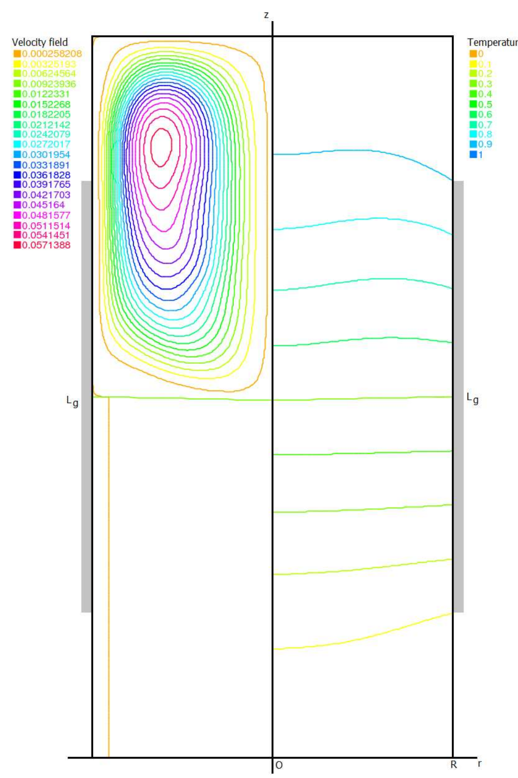

Fig. 20. Streamlines and temperature profile for $L_g = 0.750$, $Ra = 10^6$.

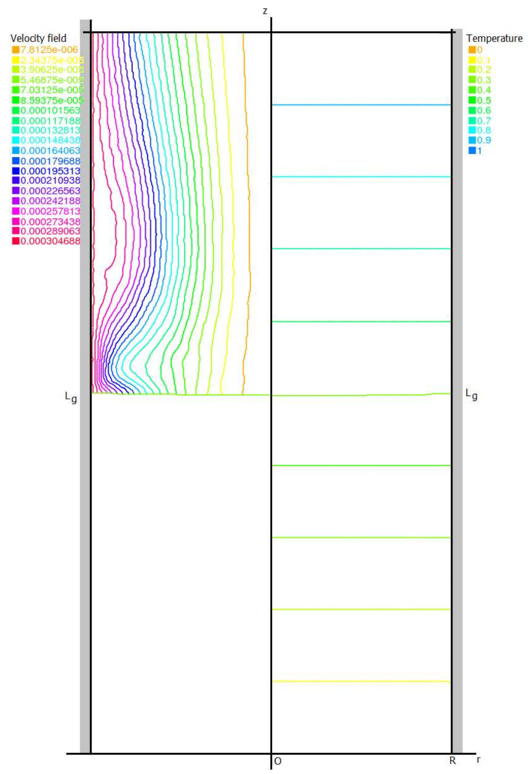

Fig. 21. Streamlines and temperature profile for $L_g = 1.000$, $Ra = 10^6$.

The deflection of the interface for the considered L_g is presented in Figure 22. This figure shows that variations of

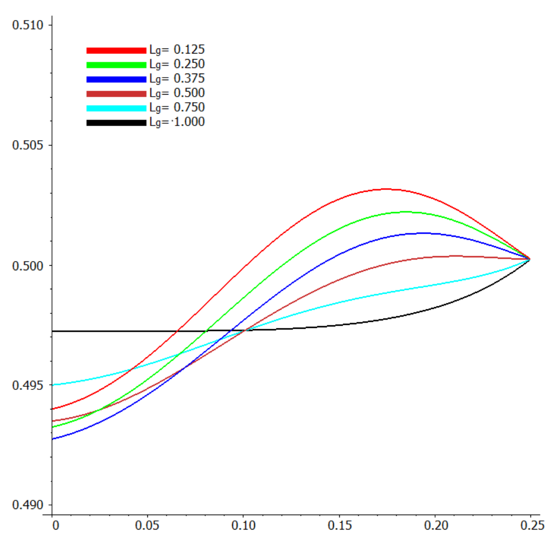

Fig. 22. The solidification interface corresponding to different values of L_g

L_g in the range $[0.125, 0.500]$ produce small variations on the melt-solid interface, but deflection of the interface is quit large. If L_g increases to 1, then the interface deflection decreases. Also, the shape of the interface changes from "S"-shape to slight-convex shape when L_g increases and, for $L_g = 1$, the interface shape tends to be flatten.

IV. CONCLUSIONS

In this paper, the influence of the temperature profile in a vertical Bridgman instalation on the fluid flow and interface deflection was studied. For all considered gravity conditions, it can be observed that the streamline amplitude decreases and the shape of the solidification interface tends to be flatten as the length of the gradient zone in the furnace increases to 1. Also, for a given length of the gradient zone, L_g, stronger gravitational forces tend to increase the amplitude of the streamlines and to flatten the isotherms in the melt. For $L_g = 1$, the gravitational field has no influence on the velocity field in the melt nor the temperature profile (and melt-solid interface) in the ampoule.

REFERENCES

[1] D. J. T. Hurle (ed.), *Handbook of crystal growth*, vol. 2A, Amsterdam Lausanne New York Elsevier, 1994

[2] P. M. Adornato, R. A. Brown, Convection and segregation in directional solidification of dilute and non-dilute binary alloys: effects of ampoule and furnace design, *Journal of Crystal Growth* 80, 1987, pp. 155-190

[3] C. J. Chang, R. A. Brown, Radial segregation induced by natural convection and melt/solid interface shape in vertical Bridgman growth, *Journal of Crystal Growth* 63, 1983, pp.343-364

[4] M. M. Mihailovici et al., The axial and radial segregation in semiconductor crystals grown by Bridgman-Stockbarger method in a low gravity environment due to the initial dopant distribution, *Proceedings of the International Conference on Homogenisation and Applications to Material Sciences*, West University Press, 2002, pp.75-86

[5] M. M. Mihailovici et al., The axial and radial segregation, due to the thermo-convection, the decrease of the melt in the ampoule and the effect of the precrystallisation zone, in the semiconductor crystals grown in a Bridgman-Stockbarger system in low gravity environment, *Journal of Crystal Growth* 237-239 P3, 2002, pp.132-136

[6] E. Tulcan-Paulescu et al., A 2-D mathematical model for a semiconductor crystal grown in strictly zero-gravity, *Proceedings of International Conference on Nonlinear Problems in Aviation and Aerospace ICNPAA 2004*, Cambridge Scientific Publishers, 2005

[7] S. Maris, A. Neculae, A.M. Balint, Numerical simulation of the solidification process for a binary alloy in a Bridgman-Stockbarger installation, *Proceedings of 9th National Conference of the Romanian Mathematical Society*, 2005

[8] S. Maris, A. Neculae, St. Balint, Determination of the thermal field, flow and concentration fields in a directional solidification system, *Proceedings of the 8th National Conference of Mathematical Analysis and Applications*, 2006

[9] S. Maris, Some properties of the stationary solution in the case of solidification using Bridgman technique, *Proceedings of 14th WSEAS International Conference on Applied Mathematics*, WSEAS Press, 2009, pp. 42-46

[10] S. Maris, Determination of the stationary solution in the case of solidification using Bridgman technique, *International Journal of Mathematical Models and Methods in Applied Sciences*, Vol. 4/1, 2010, pp.58-65

[11] S. Maris, L. Braescu, Effect of the temperature profile on the fluid flow and interface deflection in the case of crystals grown by Bridgman technique, *Proceedings of the 3rd WSEAS International Conference on Materials Science*, WSEAS Press, 2010

[12] F. Hecht, O. Pironneau, K. Ohtsuka - *FreeFem++ Manual*, version 2.11 (www.freefem.org).